

Theory on the Thermoanalytical Techniques in Differential Scanning Calorimetry. Application to the Crystallization of the Semiconducting $\text{Sb}_{0.20}\text{As}_{0.32}\text{Se}_{0.48}$ Alloy

J. Vázquez*, R. González-Palma, P. L. López-Aleman, P. Villares and R. Jiménez-Garay

Departamento de Física de la Materia Condensada, Facultad de Ciencias, Universidad de Cádiz, Apartado 40,11510, Puerto Real (Cádiz) Spain

Received September 15, 2004; accepted May 17, 2005

PACS numbers: 64.60; 64.70; S7.12; S8.12

Abstract

A procedure has been considered for analyzing the evolution with time of the volume fraction transformed and for calculating the kinetic parameters at non-isothermal reactions in materials involving formation and growth of nuclei. By assuming that the nucleation process takes place early in the transformation and the nucleation frequency is zero thereafter, “site saturation”, a general expression of the fraction transformed as a function of time has been obtained in isothermal crystallization processes. The application of the transformation rate to the non-isothermal processes has been carried out under the restriction that the quoted rate depends only on the fraction transformed and the temperature. Under this condition, the kinetic parameters have been deduced by using the techniques of data analysis of single-scan and multiple-scan. The theoretical method analyzed has been applied to the glass-crystal transformation kinetics of the semiconducting $\text{Sb}_{0.20}\text{As}_{0.32}\text{Se}_{0.48}$ alloy. The kinetic parameters obtained according to both techniques differ by only about 2.4%, which confirms the reliability and accuracy of the single-scan technique when calculating the above-mentioned parameters in non-isothermal transformation processes.

1. Introduction

The investigation of non-crystalline materials is a very active field since it promises to yield new and very good properties, offering a new field for applications. It has long been recognized that many technologically important properties of materials, such as their mechanical strength and toughness, creep and corrosion resistance, and magnetic and superconducting properties are essentially controlled by the presence of precipitated particles of a second phase [1, 2]. An important part of recent developments corresponds to nanostructured materials obtained by controlled crystallization, either by annealing the amorphous single phase or by decreasing the cooling rate from the liquid of different systems. Typically, in these processes precipitate crystalline particles arise embedded in an amorphous matrix. Differential calorimetry has become quite effective in studying the nature of the quoted structures and their stability. Accordingly, a strong theoretical and practical interest in the application of isothermal and non-isothermal experimental analysis techniques to the study of phase transformations has been developed in the last decades. The non-isothermal thermoanalytical techniques have become particularly prevalent for the investigation of the processes of nucleation and growth that occur during transformation of the metastable phases in a glassy alloy as it is heated. These techniques provide rapid information on such parameters as glass transition temperature, transformation enthalpy and activation energy over a wide range of temperatures [3]. In addition, the high thermal conductivity as well as the temperature at which transformation occurs in most amorphous alloys make these

transformations particularly suited to analysis in a Differential Scanning Calorimeter (DSC).

The study of crystallization kinetics in amorphous materials by DSC techniques has been widely discussed in the literature [4, 5]. There is a large variety of mathematical treatments mostly based on the Johnson-Mehl-Avrami (JMA) transformation rate equation [6–9]. In this work the conditions of applicability of the JMA transformation rate equation to non-isothermal crystallization are established. The kinetic parameters of the above-mentioned crystallization are deduced by using the techniques of data analysis of single-scan and multiple-scan. Finally, the present paper applies the quoted techniques to the analysis of the crystallization kinetics of the glassy alloy $\text{Sb}_{0.20}\text{As}_{0.32}\text{Se}_{0.48}$ and the values of the kinetic parameters thus obtained differ by about 2.4%. This fact shows the reliability and accuracy of the single-scan technique for the calculation of the quoted parameters from a continuous heating treatment.

2. Theory

The theoretical basis for interpreting DTA or DSC results is provided by the formal theory of transformation kinetics [6–11]. In its basic form this theory describes the evolution with time, t , of the volume fraction crystallized, x , in terms of nucleation frequency per unit volume, I_v , and crystal growth rate, u , as

$$x = 1 - \exp \left\{ -g \int_0^t I_v(\tau) \left[\int_\tau^t u(t') dt' \right]^m d\tau \right\} \quad (1)$$

when the crystal growth rate is isotropic, an assumption which is in agreement with the experimental evidence, since in many transformations the reaction product grows approximately as spherical nodules [12]. Moreover, m is an exponent related to the dimensionality of the crystal growth and the mode of transformation, g being a geometric factor, which depends on the dimensionality and shape of the crystal growth, and therefore, its dimension equation can be expressed as

$$[g] = [\text{L}]^{3-m}, \quad [\text{L}] \text{ is the length}$$

By assuming that the nucleation process takes place early in the transformation and the nucleation frequency is zero thereafter, the case referred to as “site saturation” by Cahn [13, 14], eq. (1) becomes

$$x = 1 - \exp \left[-gN \left(\int_0^t u(t') dt' \right)^m \right] = 1 - \exp(-gNI_1^n) \quad (2)$$

where N is the number of pre-existing nuclei per unit volume, $n = m$, and the growth integral is evaluated between 0 and t , since there is no nucleation period, $\tau = 0$.

*Corresponding Author Email: jose.vazquez@uca.es

Although, in general, the temperature dependence of the crystal growth rate is not Arrhenian when a broad range of temperature is considered [15], however, over a sufficiently limited range of temperature (such as the range of crystallization peaks in DSC experiments), u may be described in a zero-order approximation by

$$u \approx u_0 \exp(-E/RT) \quad (3)$$

where E is the effective activation energy for crystal growth and R is the ideal gas constant.

Taking the derivative of eq. (2) with respect to time in an isothermal process, substituting eq. (3) in the resulting expression, and eliminating the exponential function, $\exp(-gNI_1^n)$, between this expression and the quoted eq. (2), the crystallization rate is obtained as

$$\begin{aligned} \frac{dx}{dt} &= n(gN)^{1/n} u_0 [\exp(-E/RT)] (1-x) [-\ln(1-x)^{(n-1)/n}] \\ &= nK(1-x) [-\ln(1-x)]^{(n-1)/n} \end{aligned} \quad (4)$$

K being the reaction rate constant, which dimension equation is $[K] = [T^{-1}]$.

Equation (4) is sometimes referred to as the JMA transformation rate equation.

2.1. Applicability of the Johnson-Mehl-Avrami transformation rate equation under non-isothermal conditions

It was suggested by Henderson [16] in a notable paper that eq. (4) as developed by JMA is based on the following important assumptions:

1. isothermal regime;
2. spatially random nucleation;
3. growth rate of the new phase dependent only on temperature and not on time.

It has been asserted by Christian [12] that eq. (4) may be used as an approximation for the early stages of diffusion controlled growth transformation processes for which assumption 3 may not rigorously hold.

In the past decades eq. (4) has been applied without qualification to the analysis of non-isothermal phase transformations [17–19]. However, according to the literature [20], the above-mentioned equation can be rigorously applied under non-isothermal regime if it can be shown that the transformation rate depends only on the state variables x and T . Under this restriction an example of a system which allows the non-isothermal application of eq. (4) is one in which the nucleation takes place early in the transformation and the nucleation rate is zero thereafter. In addition, in cases as above-mentioned, the reaction rate constant, K , could demonstrate a simple Arrhenius behaviour, $K = K_0 \exp(-E/RT_a)$, or a Vogel-Fulcher, $K = K_0 \exp[-E/R(T_a - T_0)]$, with respect to temperature during the crystallization process. In these expressions of the rate constant, K_0 is the frequency factor, E is the overall effective activation energy, T_0 is a constant temperature, and T_a is the absolute temperature.

The analysis of crystallization kinetics is developed in terms of a generalized temperature parameter, T . The generalized formalism can be applied directly to either Arrhenius behaviour or Vogel-Fulcher behaviour by substituting T_a or $T_a - T_0$ for T , respectively. Considering the generalized temperature dependence for K , the kinetic parameters associated with the transformation process are E , n and K_0 . The techniques of data

analysis to obtain the quoted parameters can be divided into single-scan analysis and multiple-scan analysis techniques.

2.1.1. Single-scan technique. In the derivation of relationships for calculating kinetic parameters of the glass-crystal transformation by using a non-isothermal regime, a reaction rate independent of the thermal history is necessary. Thus, the reaction rate is expressed as the product of two separable functions of absolute temperature and the volume fraction transformed. In these conditions eq. (4) can be written

$$\frac{dx}{dt} = nKf(x) = nK_0f(x)[\exp(-E/RT)]. \quad (5)$$

Bearing in mind that the heating rate is $\beta = dT/dt$, eq. (5) must be integrated by separation of variables and one obtains

$$\int_0^x \frac{dx'}{(1-x')[-\ln(1-x')]^{(n-1)/n}} = \frac{nK_0}{\beta} \int_{T_0}^T e^{-E/RT'} dT' \quad (6)$$

and replacing $-\ln(1-x')$ with z' and E/RT' with y' , the integration of eq. (6) yields

$$[-\ln(1-x)]^{1/n} = \frac{K_0E}{\beta R} \int_y^\infty e^{-y'} y'^{-2} dy' = \frac{K_0E}{\beta R} I \quad (7)$$

if it is assumed that $T_0 \ll T$ (T_0 is the initial temperature of the process), so that y_0 can be taken as infinity. This assumption is justifiable for any heating treatment which begins at a temperature where nucleation and crystal growth are negligible, i.e., below glass transition temperature for most glass-forming systems [15].

The integral I is not integrable in closed form and the literature [21, 22] gives several series expansions for the quoted integral. Vázquez *et al.* [23] have developed a method to evaluate it by an alternating series, resulting in

$$I = \left[-e^{-y'} y'^{-2} \sum_{k=0}^{\infty} \frac{(-1)^k (k+1)!}{y'^k} \right]_y^\infty$$

where it is possible to use only the two first terms, without making any appreciable error and to obtain

$$I = \left(\frac{RT}{E} \right)^2 \left(1 - \frac{2RT}{E} \right) \exp(-E/RT) \quad (8)$$

Substituting this expression of I into eq. (7), and taking the logarithm of the resulting expression gives

$$\ln[-\ln(1-x)] - 2n \ln T = -\frac{nE}{RT} + n \ln \frac{K_0R}{\beta E} \quad (9)$$

if it is assumed that the term $2RT/E$ in eq. (8) is negligible in comparison to unity, since in most crystallization reactions $E/RT \gg 1$ (usually $E/RT \geq 25$) [24]. When n is known, a plot of $\ln[-\ln(1-x)] - 2n \ln T$ versus $1/T$ yields a straight line whose slope provides a value of the product nE . However, according to the literature [25] over a temperature range of 100 K the contribution of the term $2n \ln T$ can be ignored without causing a substantial error in the calculated slope.

On the other hand, taking the logarithm of eq. (5) results

$$\ln \left(\frac{dx}{dt} \right) = \ln[f(x)] + \ln(nK_0) - \frac{E}{RT}. \quad (10)$$

Hence when $\ln(dx/dt)$ is plotted versus $1/T$ a straight line is obtained, whose slope allows for the calculation of the activation energy, E , of the glass-crystal transformation, if it is assumed that for $0.25 < x < 0.75$ the function $\ln[f(x)]$ may be considered constant. Figure 1 shows a plot of $\ln[f(x)]$ versus x for $n = 2, 3$

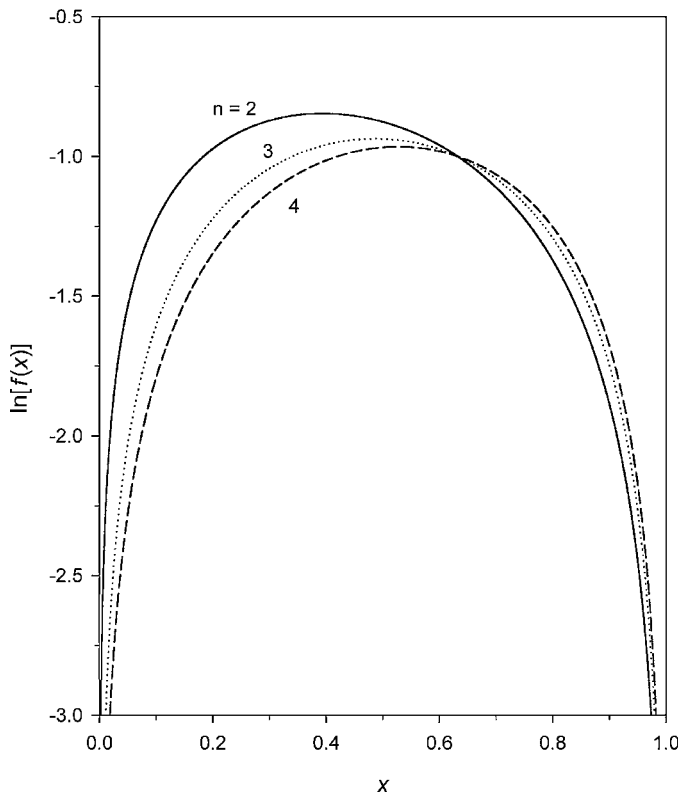


Fig. 1. Plot of $\ln[f(x)] = \ln\{(1-x)[- \ln(1-x)]^{(n-1)/n}\}$ versus x for $n = 2, 3$, and 4 .

and 4 . It should be noted that for small values of x and for values close to 1 , the function $\ln[f(x)]$ changes rapidly with x , whereas for the above quoted interval, $\ln[f(x)]$ holds practically constant. The determination of nE and E makes it possible to directly obtain the parameter n .

For those systems in which K shows Vogel-Fulcher behaviour with respect to temperature a determination of T_0 must also be made, according to Henderson [16]. In this case the effective activation energy, $E_{\text{eff}}(T_a)$, can be obtained by the relationship

$$\frac{d[\ln(dx/dt)]}{dT_a^{-1}} = \frac{E_{\text{eff}}(T_a)}{R}. \quad (11)$$

The derivative of eq. (10) with respect to T_a^{-1} leads to the expression

$$\frac{d[\ln(dx/dt)]}{dT_a^{-1}} = -\frac{E}{R} \left(\frac{T_a}{T_a - T_0} \right)^2 - nK_0 \frac{T_a^2}{\beta} \frac{d[f(x)]}{dx} \times \exp[-E/R(T_a - T_0)].$$

Considering the negligible exponential term, and equating the resulting expression with eq. (11), yields

$$E_{\text{eff}}(T_a) [(T_a - T_0)/T_a]^2 \approx -E = \text{const}$$

and measuring $E_{\text{eff}}(T_a)$ at two widely spaced temperatures T_{a1} and T_{a2} the value of T_0 can be determined as

$$T_0 = (AT_{a1} - T_{a2})(A - 1)^{-1} \quad (12)$$

with $A = T_{a2}T_{a1}^{-1} \{E_{\text{eff}}(T_{a1})[E_{\text{eff}}(T_{a2})]^{-1}\}^{1/2}$.

This value of T_0 substituted in T should produce a linear behaviour of eqs. (9) and (10) for the determination of nE and E , respectively.

Finally, after E , n and T_0 have been determined, the frequency factor, K_0 , can be obtained from the maximum transformation

rate, which is found by making $d^2x/dt^2 = 0$, and according to eqs. (4) and (5) one obtains

$$\frac{\beta E}{RT_p^2} = nK_p \left\{ [- \ln(1 - x_p)]^{(n-1)/n} - \frac{n-1}{n} [- \ln(1 - x_p)]^{-1/n} \right\} \quad (13)$$

where the subscript p denotes the quantity values corresponding to the maximum transformation rate. By using eqs. (7) and (8) and assuming again that the term $2RT_p/E \ll 1$ into eq. (13) results in that $K_p = \beta E(RT_p^2)^{-1}$ and $- \ln(1 - x_p) = 1$ or $x_p = 0.63$, independent of β or n . Accordingly, from eq. (5) results in the following expression

$$K_0 = (dx/dt)|_p [0.37n \exp(-E/RT_p)]^{-1} \quad (14)$$

for the frequency factor.

2.1.2. Multiple-scan technique. The single-scan analysis techniques outlined above is predicated on a detailed knowledge of the functional dependence of the transformation rate, dx/dt , on the fraction transformed, x , and the generalized temperature, T . The multiple-scan rate analysis techniques do not depend on a specific knowledge of the dependence of dx/dt on x . The procedure requires the characterization of the transformation by using several scan rates. When this procedure is applied to the case of a JMA transformation rate equation, the use of eq. (2) for the treatment of non-isothermal experiments is interesting. The maximum transformation rate is found making $d^2x/dt^2 = 0$, thus obtaining the relationship

$$nC_p (I_1^n)|_p = \beta E (I_1)|_p (RT_p^2)^{-1} + (n-1)u_p \quad (15)$$

where $C_p = gNu_p$, and its dimension equation can be expressed as

$$[C_p] = [L]^{1-n} [T]^{-1}.$$

According to eqs. (2), (6) and (7) one obtains

$$(I_1)|_p = \frac{u_0 E I_p}{\beta R} = \frac{u_0 E}{\beta R} \int_{y_p}^{\infty} e^{-y} y^{-2} dy$$

an expression that bearing in mind eq. (8) becomes in the relationship

$$(I_1)|_p = \frac{u_0 R}{\beta E} T_p^2 \left(1 - \frac{2RT_p}{E} \right) \exp(-E/RT_p) \quad (16)$$

that when it is inserted into eq. (15) results in $(I_1)|_p = (gN)^{-1/n} (1 - 2RT_p/nE)^{1/n}$. When both expressions for $(I_1)|_p$ are equated, one obtains a relationship whose logarithmic form can be written as

$$\ln(T_p^2/\beta) + \ln(K_0 R/E) - E/RT_p \approx (2RT_p/E)(1 - n^{-2}) \quad (17)$$

where the function $\ln(1 - v)$ with $v = 2RT_p/nE$ or $v = 2RT_p/E$ is expanded as a series and has been taken as only the first term of itself.

Note that, for most crystallization reactions, the right hand side (RHS) of eq. (17) is generally negligible in comparison to the individual terms on the left-hand side for common heating rates ($\leq 100 \text{ K min}^{-1}$), thus for $n > 1$ and $E/RT_p > 25$ the error introduced in the value of E/R is less than 1%. Equation (17) serves to determine the activation energy, E , and the frequency factor, K_0 , from the slope and intercept, respectively, of the $\ln(T_p^2/\beta)$ versus $1/T_p$ plot.

Finally, it should be noted that eq. (17) with RHS = 0 is obtained considering that $2RT_p/E \ll 1$, according to the literature [24], and therefore, $(I_1)|_p = (gN)^{-1/n}$. Thus, taking the

derivative of eq. (2) with respect to time and considering eq. (16) permits us to obtain

$$n = \frac{dx}{dt} \bigg|_p RT_p^2 (0.37\beta E)^{-1} \quad (18)$$

which makes it possible to calculate the kinetic exponent n in a set of exotherms taken at different heating rates and the corresponding mean value represents the most probable value of the kinetic exponent of the glass-crystal transformation.

3. Experimental details

The semiconducting $\text{Sb}_{0.20}\text{As}_{0.32}\text{Se}_{0.48}$ glassy alloy was made in bulk form, from components with 99.999% purity, which were pulverized to less than $64\ \mu\text{m}$, mixed in adequate proportions, and introduced into a quartz ampoule (6 mm diameter). The content of the ampoule (7 g total) was sealed at a pressure of 10^{-2} Pa with an oxyacetylene burner. The quoted ampoule was put into a furnace at 1223 K for 24 h, turning at 1/3 rpm, in order to ensure the homogeneity of the molten material. The capsule was then immersed in a receptacle containing water in order to solidify the material quickly, avoiding the crystallization of the compound. The capsule containing the sample was then put into a mixture of hydrofluoric acid and hydrogen peroxide in order to corrode the quartz and make it easier to extract the alloy. The glassy state of the material was confirmed by a diffractometric X-ray scan, in a Siemens D500 diffractometer, showing an absence of peaks, which are characteristic of crystalline phases. The homogeneity and composition of the sample was verified through Scanning Electron Microscopy (SEM) in a Jeol, scanning microscope JSM-820. The calorimetric measurements were carried out in a Perkin Elmer DSC7 differential scanning calorimeter with an accuracy of ± 0.1 K. A constant $60\ \text{ml min}^{-1}$ flow of nitrogen was maintained in order to provide a constant thermal blanket within the DSC cell, thus eliminating thermal gradients and ensuring the validity of the applied calibration standard from sample to sample. Moreover, the nitrogen purge allows to expel the gases emitted by the reaction, which are highly corrosive to the sensory equipment installed in the DSC furnace. The calorimeter was calibrated for each heating rate, using the well-known melting temperatures and melting enthalpies of high purity zinc and indium supplied with the instrument. The analyzed samples, were pulverized (particle size around $40\ \mu\text{m}$), crimped into aluminium pans, and their masses were kept about 20 mg. An empty aluminium pan was used as reference. The crystallization experiments were carried out through continuous heating at rates, β , of 1, 2, 4, 8, 16, 32 and $64\ \text{K min}^{-1}$. The glass transition temperature was considered as a temperature corresponding to the inflection point of the lambda-like trace on the DSC scan, as shown in Fig. 2. Moreover, it should be noted that the transformed fraction, x , at any temperature, T , is given as $x = A_T/A$, where A is the total area of the exotherm between the temperature T_i , where the crystallization just begins and the temperature T_f , where the crystallization is completed and A_T is the area between the initial temperature and a generic temperature, see Fig. 2.

4. Results and discussion

The typical DSC trace of $\text{Sb}_{0.20}\text{As}_{0.32}\text{Se}_{0.48}$ chalcogenide glass obtained at a heating rate of $8\ \text{K min}^{-1}$ and plotted in Fig. 2 make it possible to determine the glass transition temperature, $T_g = 456.9\ \text{K}$, the extrapolated onset crystallization temperature,

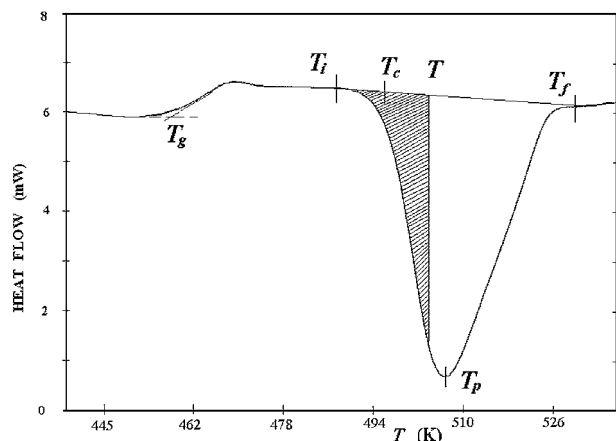


Fig. 2. Typical DSC trace of $\text{Sb}_{0.20}\text{As}_{0.32}\text{Se}_{0.48}$ glassy alloy at a heating rate of $\beta = 8\ \text{K min}^{-1}$. The hatched area shows A_T , the area between T_i and T .

$T_c = 495.8\ \text{K}$, and the peak temperature of crystallization $T_p = 507.1\ \text{K}$, of the above mentioned chalcogenide glass. This DSC trace shows the typical behaviour of a glass-crystal transformation. The thermograms for the different heating rates, β , quoted in Section 3, show values T_g , T_c and T_p which increase with increasing β , a property which has been widely quoted in the literature [24].

4.1. Crystallization

The kinetic analysis of the crystallization reactions is related with the knowledge of the reaction rate constant as a function of the temperature. In this work it is assumed that the above-mentioned constant shows an Arrhenius-type temperature dependence. In order for this assumption to hold, according to the literature [15], one of the following two sets of conditions should apply:

- The crystal growth rate, u , has an Arrhenian temperature dependence; and over the temperature range where the thermoanalytical measurements are carried out, the nucleation frequency is negligible (i.e., the condition of the "site saturation").
- Both the crystal growth and the nucleation frequency have Arrhenian temperature dependences.

In the present work the first condition is assumed in order to apply the JMA equation under a regime of continuous heating. From this point of view, the crystallization kinetics of the $\text{Sb}_{0.20}\text{As}_{0.32}\text{Se}_{0.48}$ alloy has been analyzed by using the calorimetric techniques of single-scan and multiple-scan.

With the aim of analyzing the above-mentioned kinetics, the variation intervals of the quantities described by the thermograms for the different heating rates, quoted in Section 3 are obtained and given in Table I, where T_i and T_p are the temperatures at which

Table I. The characteristic temperatures and enthalpies of the crystallization processes of alloy $\text{Sb}_{0.20}\text{As}_{0.32}\text{Se}_{0.48}$.

Parameter	Experimental value
T_g (K)	443.4–464.6
T_i (K)	471.4–507.8
T_p (K)	491.1–536.1
ΔT (K)	27.7–63.6
ΔH (mcal mg^{-1})	11.5–12.9

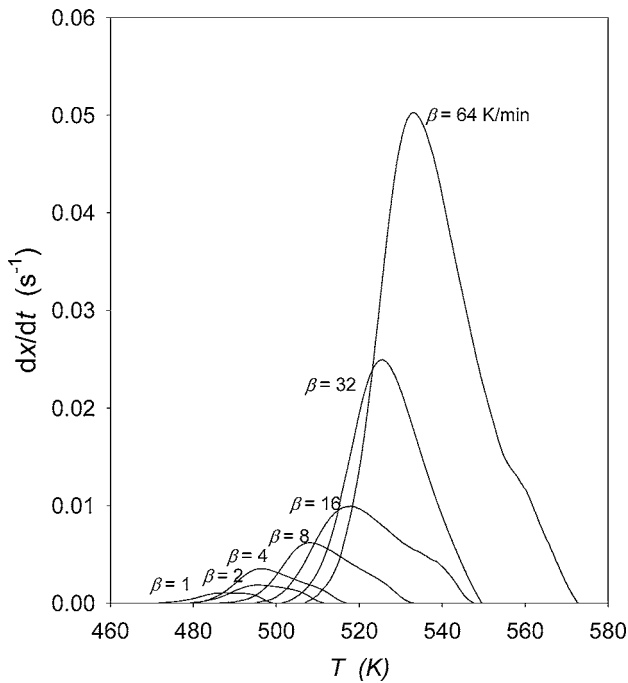


Fig. 3. Crystallization rate versus temperature of the exothermal peaks, at different heating rates.

crystallization begins and that corresponding to the maximum crystallization rate, respectively, and ΔT is the width of the peak. The crystallization enthalpy, ΔH , is also determined for each heating rate.

The ratio between the ordinates and the total area of the peak gives the corresponding crystallization rates, which makes it possible to build the curves of the exothermal peaks represented as in Fig. 3. It may be observed that the $(dx/dt)_p$ values increase in the same proportion that the heating rate, a property which has been widely discussed in the literature [26].

The single-scan technique was applied to several sets of experimental data (Table II) obtained for all heating rates, quoted in Section 3, and the results for nE from eq. (9), E from eq. (10), n derived therefrom and K_0 are included in Table II. The mean values for these parameters are: $\langle E \rangle = 45.8 \text{ kcal mol}^{-1}$, $\langle n \rangle = 1.73$ and $\langle K_0 \rangle = 3.66 \times 10^{17} \text{ s}^{-1}$. To illustrate the above-mentioned technique, Fig. 4 shows the plots of $\ln[-\ln(1-x)]$ versus $1/T$ for $\beta = 8 \text{ K min}^{-1}$, together with the corresponding straight regression line, while the plots of $\ln(dx/dt)$ versus $1/T$ with the straight regression line carried out, are shown in Fig. 5.

On the other hand, the multiple-scan technique, which allows E to be quickly evaluated, has been used to analyze the

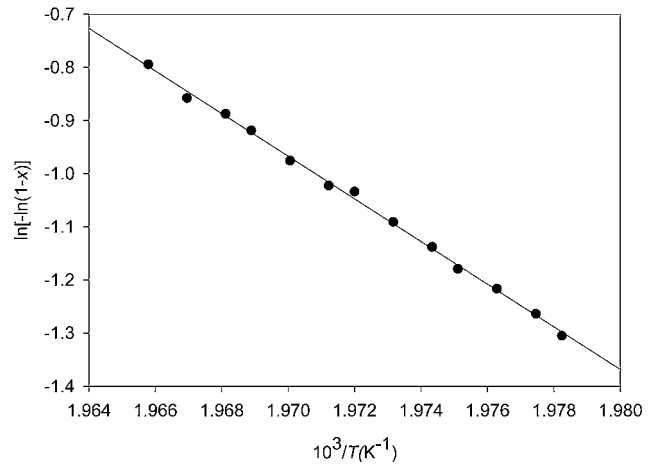


Fig. 4. Variation of $\ln[-\ln(1-x)]$ with $1/T$ for heating rate of 8 K min^{-1} .

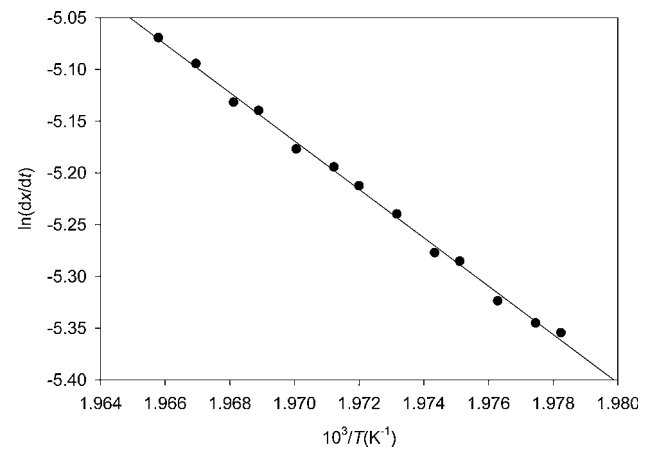


Fig. 5. Experimental plots of $\ln(dx/dt)$ versus $1/T$ and straight regression line of the $\text{Sb}_{0.20}\text{As}_{0.32}\text{Se}_{0.48}$ alloy.

crystallization kinetics of the semiconducting $\text{Sb}_{0.20}\text{As}_{0.32}\text{Se}_{0.48}$ alloy. The plots of $\ln(T_p^2/\beta)$ versus $1/T_p$ at each heating rate, and the straight regression line carried out are shown in Fig. 6. The results for E and K_0 from eq. (17) are also given in Table II.

By using the values of the maximum crystallization rates, $(dx/dt)_p$, and the temperatures, T_p , which correspond to the quoted maximum values, given in Table II, it is possible to obtain, through eq. (18), the kinetic exponent of the process corresponding to each of experimental heating rates. The values of the n parameter are also given in above-mentioned Table II. Bearing in mind that the calorimetric analysis is an indirect method which makes it possible to obtain mean values for

Table II. Kinetic parameters found for the crystallization $\text{Sb}_{0.20}\text{As}_{0.32}\text{Se}_{0.48}$ alloy by using the single-scan and multiple-scan techniques

β K min^{-1}	single-scan				multiple-scan							
	interval $T(\text{K})$	x	$10^3(dx/dt)(\text{s}^{-1})$	nE kcal mol^{-1}	E kcal mol^{-1}	n	$K_0(\text{s}^{-1})$	$T_p(\text{K})$	$10^3(dx/dt)_p$ (s^{-1})	n	E kcal mol^{-1}	$K_0(\text{s}^{-1})$
1	484.1–487.9	0.2337–0.3923	0.80–1.15	77.9	45.8	1.70	3.81×10^{17}	491.2	1.18	2.05		
2	491.3–495.0	0.2514–0.4067	1.34–1.89	77.5	45.3	1.71	1.93×10^{17}	495.8	1.96	1.73		
4	497.5–499.1	0.2654–0.3276	3.20–3.70	78.3	45.0	1.74	1.87×10^{17}	499.8	3.72	1.67		
8	505.5–508.7	0.2396–0.3636	4.71–6.30	80.5	46.8	1.72	8.09×10^{17}	508.6	6.32	1.47	45.1	1.83×10^{17}
16	513.0–516.2	0.2368–0.3541	10.21–13.51	79.6	46.3	1.72	4.89×10^{17}	516.5	13.59	1.63		
32	522.2–525.7	0.2475–0.3772	19.48–26.12	80.0	46.0	1.74	3.50×10^{17}	526.0	26.22	1.63		
64	530.9–535.9	0.1896–0.3443	34.09–50.76	79.3	45.3	1.75	1.53×10^{17}	536.2	51.07	1.65		

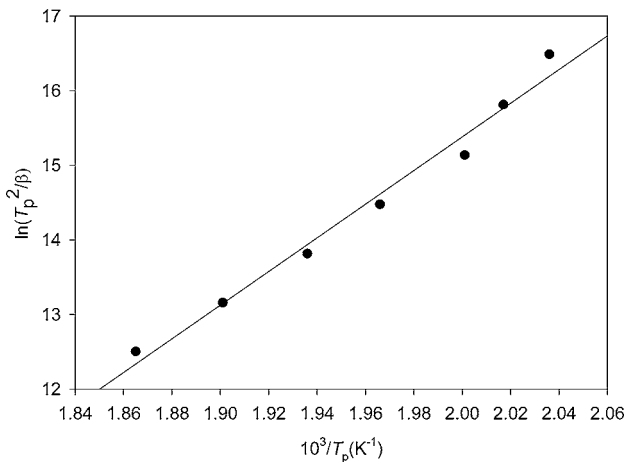


Fig. 6. Plots of $\ln(T_p^2/\beta)$ versus $1/T_p$ of the analyzed material (β in Ks^{-1}).

the parameters that control the kinetics of a reaction, the corresponding mean value, $\langle n \rangle = 1.69$, has been calculated.

With the aim of correctly analyzing the reliability of the single-scan technique, when calculating kinetic parameters in non-isothermal crystallization processes, the values of the above parameters E , n and $\ln K_0$, calculated by means of the above-mentioned technique, are compared with its values obtained through the multiple-scan technique, Table II, finding that the error between them for the less accurate parameter is less than 2.4%. This result is in agreement with the literature [19], where it is shown that for $(n-1)/n = 0.6$ in the range of $0.2 < x < 0.4$ results in an error of 7% in the calculated slope E/R , an error acceptable in most crystallization reactions.

Considering that the crystallization process of the studied material is basically a growth of the pre-existing nuclei in the as-quenched glass, from the value of the kinetic exponent, $n = 1.73$, and according to the Avrami theory of crystal growth, it is possible to state the fact that in the crystallization reaction mechanism there is a diffusion-controlled growth, coherent with the basic formalism used. According to the literature [27] the transformed phase may exhibit in an initial growth of particles nucleated at a constant rate, since the mean value of the kinetic exponent is included in the interval 1.5–2.5.

For the unambiguous interpretation of $n = 1.73$ as a consequence of a diffusion-controlled crystallization, it is recommended to try to identify the possible phases that crystallize in the material after the thermal treatment by means of adequate X-ray diffraction measurements. The diffractograms for as-quenched glass and for the material after the overall crystallization are shown in Fig. 7. Trace (A) shows broad humps characteristic of the amorphous state of the starting material. The diffractogram of the transformed material suggests the presence of microcrystallites of Sb_2Se_3 , AsSe and As_2Se_3 indicated in the trace (B) with \bullet , \circ and $\#$, respectively, together with elemental crystalline Se , remaining a residual amorphous matrix. The quoted phases Sb_2Se_3 and AsSe crystallize in the orthorhombic and monoclinic systems [28] with unit cells defined by $a_1 = 11.633 \text{ \AA}$, $b_1 = 11.78 \text{ \AA}$, $c_1 = 3.895 \text{ \AA}$ and $a_2 = 9.527 \text{ \AA}$, $b_2 = 13.86 \text{ \AA}$, $c_2 = 6.69 \text{ \AA}$, $\alpha = \beta = 90^\circ$, $\gamma = 106.18^\circ$, respectively.

5. Conclusions

The described theoretical procedure enables us to study the evolution with time of the volume fraction transformed in

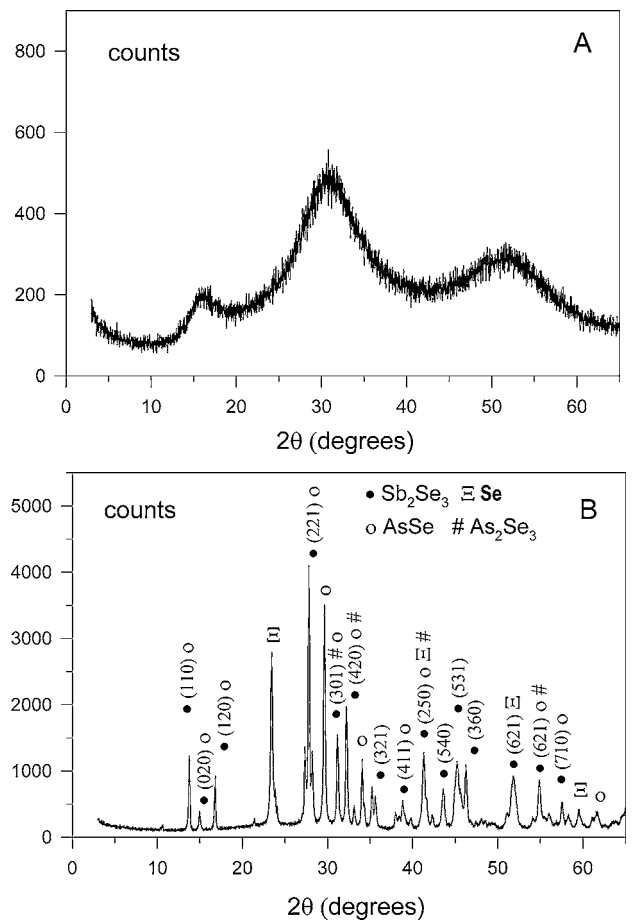


Fig. 7. (A) Diffractogram of the amorphous $\text{Sb}_{0.20}\text{As}_{0.32}\text{Se}_{0.48}$ alloy. (B) Diffraction peaks of the alloy crystallized in DSC.

materials involving nucleation and crystal growth processes. This method assumes that the nucleation process takes place early in the transformation and the nucleation frequency is zero thereafter, “site saturation”. By using this assumption a general expression for the transformed fraction as a function of time in bulk crystallization processes has been obtained. In the case of isothermal transformation, the above-mentioned expression has been transformed in an equation, which can be taken as a specific case of the JMA transformation equation. The application of this equation to non-isothermal transformations implies restrictive conditions as it is the case of a transformation rate, which depends only on the fraction transformed and the temperature. Under this restriction the kinetic parameters have been deduced both for the single-scan technique and for the multiple-scan technique, which are applicable to constant scan rate DTA and DSC experiments on materials which obey the JMA transformation rate equation.

The above-mentioned techniques have been applied to the crystallization kinetics of the semiconducting $\text{Sb}_{0.20}\text{As}_{0.32}\text{Se}_{0.48}$ alloy. The difference between the obtained values for the kinetic parameters by means of both techniques is less than 2.4%. This good agreement shows the reliability of the single-scan technique for the calculation of kinetic parameters, mainly in the interval (0.2–0.4) of the volume fraction crystallized is a fact in agreement with the literature.

Acknowledgments

The authors are grateful to the Junta de Andalucía and the CICYT (Comisión Interministerial de Ciencia y Tecnología), project no. MAT 2001-3333 for their financial support.

References

1. Wagner, R. and Kampmann, R., "Phase transformations in materials" (edited by R. W. Cahn, P. Haasen and E. J. Kramer) (Mater. Sci. and Tech VCH 1991) vol. 5, p. 213.
2. McHenry, M. E., Willard, M. A. and Laughlin, D. E., *Progr. Mater. Sci.* **44**, 291 (1999).
3. Altounian, Z. and Strom-Olsen, J. O., "Thermal Analysis in Metallurgy". (Edited by R. D. Shull and A. Joshi) (Warrendale, P. A. 1992) p. 155.
4. Kelton, K. F., "Crystal Nucleation in Liquids and Glasses" (Academic Press New York 1991) *Solid State Phys.*, Vol. 45.
5. Clavaguera, N., *J. Non-Cryst. Solids* **162**, 40 (1993).
6. Avrami, M., *J. Chem. Phys.* **7**, 1103 (1939).
7. Avrami, M., *J. Chem. Phys.* **8**, 212 (1940).
8. Avrami, M., *J. Chem. Phys.* **9**, 177 (1941).
9. Weinberg, M. C. and Kapral, R., *J. Chem. Phys.* **91**, 7146 (1989).
10. Johnson, W. A. and Mehl, K. F., *Trans. Am. Inst. Mining, Met. Eng.* **135**, 315 (1981).
11. Kolmogorov, A. N., *Bull. Acad. Sci. USSR (Sci. Mater. Nat.)* **3**, 3551 (1937).
12. Christian, J. W., "The Theory of Transformations in Metals and Alloys" (Pergamon Press New York 1975).
13. Cahn, J. W., *Acta Metal.* **4**, 573 (1956).
14. Cahn, J. W., *Acta Metal.* **4**, 449 (1956).
15. Yinnon, H. and Uhlmann, D. R., *J. Non-Cryst. Solids* **54**, 253 (1983).
16. Henderson, D. W., *J. Non-Cryst. Solids* **30**, 301 (1979).
17. Skvara, F. and Satava, V., *J. Therm. Anal.* **2**, 325 (1970).
18. Sestak, J., *Thermochim. Acta* **3**, 1 (1971).
19. Sestak, J., *Phys. Chem. Glasses* **6**, 137 (1974).
20. Kemény, T., *Thermochim. Acta* **110**, 131 (1987).
21. Murray, P. and White, J., *Trans. Brit. Ceram. Soc.* **54**, 204 (1955).
22. Doyle, C. D., *Nature* **207**, 290 (1965).
23. Vázquez, J., Wagner, C., Villares, P. and Jiménez-Garay, R., *Acta Mater.* **44**, 4807 (1996).
24. Vázquez, J., Wagner, C., Villares, P. and Jiménez-Garay, R., *J. Non-Cryst. Solids* **235–237**, 548 (1998).
25. Sestak, J., *Thermochim. Acta* **3**, 150 (1971).
26. Gao, Y. Q., Wang, W., Zheng, F. Q. and Liu, X., *J. Non-Cryst. Solids* **81** 135 (1986).
27. Rao, C. N. R. and Rao, K. J., "Phase Transition in Solids" (Mc Graw Hill, New York 1978).
28. Demboski, S. A., *Russ. J. Inorg. Chem. (Engl. transl.)* **8**, 798 (1963).